ELSEVIER

Thin Solid Films 257 (1995) 166–184

Thin Solid Films

# Electrochemistry of fullerene films

Jerzy Chlistunoff, David Cliffel, Allen J. Bard *

*Department of Chemistry and Biochemistry, The University of Texas at Austin, Austin, TX 78712, USA*

**Abstract**

The preparation of $C_{60}$ films on electrodes by drop coating, Langmuir–Blodgett and electrochemical techniques, and the electrochemical behavior of these films in acetonitrile solutions containing a variety of supporting electrolytes (e.g., quaternary ammonium, alkali metal, and alkaline earth salts) is reviewed. Reduction can form insoluble films with incorporated cations or lead to dissolution. The large splitting between cathodic and anodic waves is discussed in terms of structural rearrangements during the redox processes. Studies of $C_{60}$ electrodes with the quartz crystal microbalance and with the scanning electrochemical microscope, and by laser-desorption mass spectrometry and surface-enhanced Raman scattering are also discussed.

*Keywords:* Electrochemistry; Fullerenes; Interfaces; Phase transitions

## 1. Introduction

The electrochemistry of the fullerenes, e.g. $C_{60}$, is of interest because it provides information about the energetics and kinetics of electron-transfer processes and chemical reactions associated with them. Thus, studies of the reduction of $C_{60}$ in solvents where it is moderately soluble (e.g., toluene, *o*-dichlorobenzene) [1–3] produces a series of (up to six) diffusion-controlled, nernstian reduction waves showing the successive addition of electrons to the molecule (Fig. 1).

$$C_{60}^{n-} + e^- \rightleftarrows C_{60}^{(n+1)-}; \quad n = 0, 1, \ldots, 5 \qquad (1)$$

The first oxidation step of dissolved $C_{60}$ shows an irreversible multielectron wave in these solvents, probably because of the instability of $C_{60} \cdot ^+$. This species can be detected by mass spectrometry and electrochemically in other solvents (tetrachloroethylene) [4], however. The first experiments with films of $C_{60}$ in solvents like acetonitrile [5], in which $C_{60}$ shows negligible solubility, were undertaken to investigate the energetics of the electron-transfer reaction, to judge the feasibility of electrochemical doping (i.e. the introduction of cations during reduction for charge compensation), and to learn whether the oxidized $C_{60}$ species is more stable under these conditions. The $C_{60}$ films were shown to exhibit more complicated electrochemical behavior, as discussed below, suggesting large structural changes on reduction and cation doping.

Electrochemical reduction of fullerene films is of interest because it provides a straightforward and accurate way to control the reduction level of the material, e.g. in studies of film conductivity. It also allows doping with a large array of cations, e.g. quarternary ammonium and other organic species, that are not conveniently accessible by vacuum evaporation methods. Such solution-phase electrochemical doping is often complicated, however, by the fact that solvation of the $C_{60}$ and the dopant cations produces "solvent-wet" films.

Interpretation of the electrochemical, usually cyclic voltammetry (CV), results is complicated by the extent and rate of dissolution of reduced forms of the fullerenes. In solvents in which $C_{60}$ is soluble, reduced forms often produce supersaturated solutions and hence show solution-like (i.e. diffusional) behavior. On the other hand, in studies of $C_{60}$ films, reduced species may undergo dissolution slowly, leading to CV responses characteristic of both surface and diffusional species. The fact that reduced species are soluble in some solvents in which the parent $C_{60}$ is not can be exploited to

*Corresponding author.

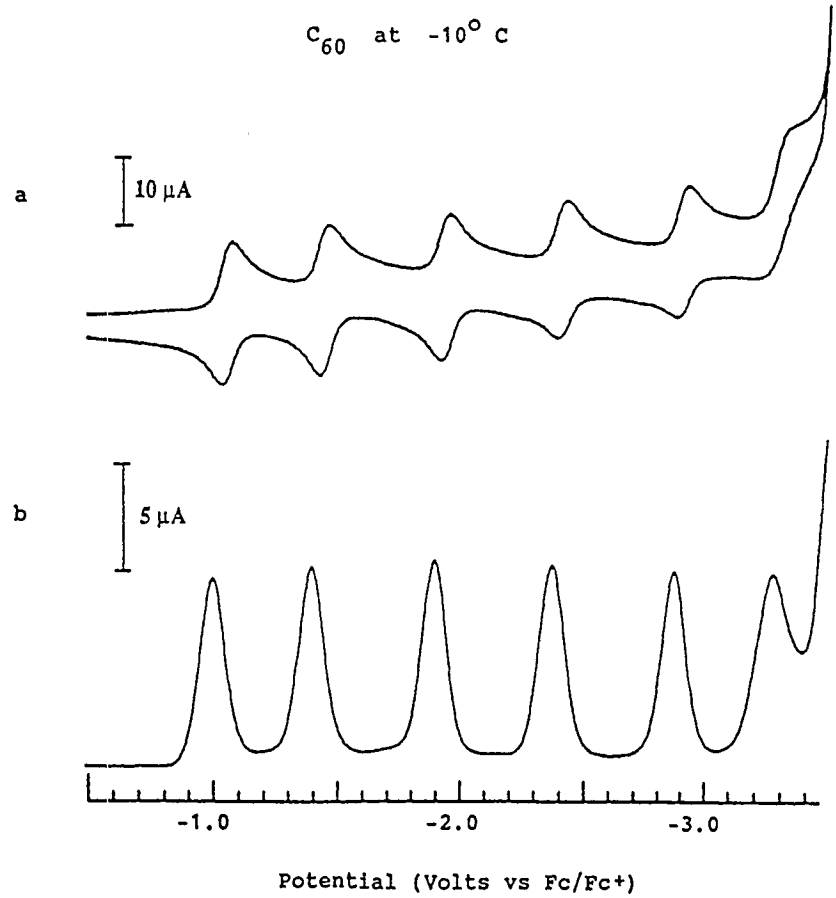


Fig. 1. Reduction of $C_{60}$ in MeCN/toluene (1:5.4 by volume) at −10 °C using (a) cyclic voltammetry, 100 mV $s^{-1}$ scan rate, and (b) differential pulse voltammetry, 50 mV pulse, 50 ms pulse width, 3000 ms period, 25 mV $s^{-1}$ scan rate. Reprinted with permission from Ref. [2]. Copyright 1992 American Chemical Society.

produce $C_{60}$ films electrochemically by oxidation of the reduced species. There is some evidence, as discussed below, that such films are not only solvated but may contain extraneous supporting electrolyte as well.

We review below the studies that have been carried out on the preparation (Section 2) and CV (Section 3) of several types of fullerene films. An understanding of the electrochemical behavior is aided by associated studies, e.g. with the quartz crystal microbalance and other techniques discussed in Section 4. These are then used to form an overall picture, still incomplete, of the solubility and electrolyte effects on reduced fullerene films (Section 5) and some possible electrochemical applications of these (Section 6).

## 2. Preparation of films for electrochemical studies

### 2.1. Drop coating

Because of its simplicity, drop coating has been the most commonly used technique for preparation of $C_{60}$ (and $C_{70}$) films for electrochemical studies [5–15]. The method is based on evaporation on an electrode surface of a known volume of the fullerene solution in an organic solvent. The solvents for this purpose are those in which the solubility of $C_{60}$ is relatively high, such as benzene [5–7, 10, 11], dichloromethane [5, 6, 8, 9, 12, 13], or toluene [6, 14, 15]. Scanning tunneling microscopic and scanning electrochemical microscopic studies revealed non-uniformity of such films on both nanometer and micrometer scales [6]. Significant porosity is a typical property of the solution-cast films as well, as indicated by voltammetric [6, 13] and photoelectrochemical [11] experiments. These findings are in line with the expected formation of small $C_{60}$ crystallites during evaporation of a solvent [16]. Accordingly, all of the factors that affect the rate of nucleation and crystallization, e.g. the rate of solvent evaporation, the solution concentration, and the roughness of the electrode surface, are expected to influence the morphology, topography, and mechanical stability of the film. For instance, Compton et al. [13] claim that rapid evaporation of a $C_{60}$ solution in methylene chloride, achieved using a hot-air gun, resulted in better reproducibility of the electrochemical results. The chemical composition of the film may also depend to some extent on the casting conditions, since solvents appear to be trapped in the $C_{60}$ phase [17, 18].

### 2.2. Langmuir–Blodgett techniques

Formation of high-quality Langmuir–Blodgett (LB) films of pure $C_{60}$ is difficult [6, 19]. This is because of (i) the tendency of $C_{60}$ Langmuir films to form multilayers or even crystal-like aggregates [6, 19], most probably due to the rather hydrophobic nature of $C_{60}$ molecules and a possible interaction between them and the residual solvent adsorbed [19], and (ii) the weak hydrophobicity of the most commonly used electrode materials, including highly oriented pyrolytic graphite (HOPG), polycrystalline Pt and Au, indium tin oxide (ITO), and glassy carbon [6].

Stability of the Langmuir films and the film transfer quality were significantly improved in the presence of eicosanoic (arachidic) acid [19]. In mixed $C_{60}$/arachidic acid films, $C_{60}$ molecules reside most probably in the hydrocarbon environment of the arachidic acid tails [19]. A different approach was presented by Goldenberg et al. [20], who, instead of using long-chain fatty acids to immobilize $C_{60}$ on an electrode surface by LB techniques, used substituted 1-tert-butyl-1,9-dihydrofullerene-60. The derivatized $C_{60}$ films transferred better to the hydrophobic surfaces. More hydrophobic surfaces were produced by modification of a polycrystalline gold electrode with alkyl thiols or iodine or a single-crystal Pt electrode with iodine, and these were used to obtain significant improvement in the quality of transferred pure $C_{60}$ Langmuir films [6, 19].

### 2.3. Electrochemical deposition methods

Any significant difference in solubilities of $C_{60}$ and salts containing $C_{60}$ anions in any solvent can, in principle, be employed as the basis for an electrochemical method of preparation of $C_{60}$ or reduced $C_{60}$ salt films. Among reported electrochemical filming phenomena are the following.

(1) In acetonitrile (MeCN), the formation of pure $C_{60}$ [21, 22] films upon reoxidation of electrochemically generated $C_{60}^{2-}$ or $C_{60}^{3-}$ in the presence of a variety of supporting electrolytes, formation of $(TBA^+)(C_{60}^-)$ and $(TBA^+)_2(C_{60}^{2-})$ films during oxidation of $C_{60}^{3-}$ in a $(TBA)ClO_4$ solution [22], $(Cs^+)_3(C_{60}^{3-})$ film deposition upon reduction of $C_{60}^{2-}$ in the presence of $CsAsF_6$ electrolyte [22], and presumably $(Ca^{2+})(C_{60}^-)_2$ film formation upon oxidation of $C_{60}^{2-}$ in the presence of $Ca(PF_6)_2$ electrolyte [22] (TBA = tetrabutylammonium).

(2) In methylene chloride, the formation of solid $(Ru(bpy)_3^{2+})(C_{60}^-)_2$ and presumably $(Ru(bpy)_3^{2+})(C_{60}^{2-})$ upon reduction of dissolved $C_{60}$ in the presence of $Ru(bpy)_3(PF_6)_2$ electrolyte [23] (bpy = bipyridine).

(3) In dichlorobenzene, the deposition of tetraphenylphosphonium and tetraphenylarsonium halide double salts of $C_{60}^-$ (and $C_{70}^-$) upon reduction of the fullerene in the presence of the corresponding tetraphenylarsonium or tetraphenylphosphonium halides [24].

(4) In liquid ammonia, the formation of $C_{60}$ films by oxidation of $C_{60}^-$ in KI electrolyte [25]. A film of the $K^+$ salt of $C_{60}^{5-}$ could also be produced by reduction of the soluble $C_{60}^{4-}$ species.

Only two of the processes mentioned above, however, were intended to study film production and can be recommended as film preparation techniques. These are $C_{60}$ film formation upon reoxidation of $C_{60}^{3-}$ in an MeCN/$(TBA)ClO_4$ solution [21, 22] and $(Cs^+)_3(C_{60}^{3-})$ film formation upon reduction of $C_{60}^{2-}$ in an MeCN solution of $CaAsF_6$ [22]. In both cases, the $C_{60}$ anions were generated by an exhaustive electrolysis of the $C_{60}$ suspension at a potential corresponding to the respective anion formation, i.e. at $-1.6$ and $-1.2$ V vs. SCE, respectively [21, 22]. The $C_{60}$ films were generated potentiostatically at $-0.2$ [21] or 0.0 V [22] vs. SCE. Films prepared in this way contain pure $C_{60}$ as long as the deposition current is kept sufficiently low, since the relatively high electrical resistance of a pure $C_{60}$ film produces a significant ohmic drop that can make the actual electrode potential more negative. Under such conditions, some contribution from the $(TBA^+)(C_{60}^-)$ deposition is observed [22]. Due to the negligible solubility of $C_{60}$ in MeCN, the amount of $C_{60}$ deposited, and hence the film thickness, can be calculated directly from the electrolysis charge [22]. $(Cs^+)_3(C_{60}^{3-})$ can be quantitatively synthesized by the oxidation of $C_{60}^{2-}$ at $-1.6$ V vs. SCE, as confirmed by the controlled potential coulometry at a Pt gauze electrode and electrochemical quartz crystal microbalance experiments employing a quartz/gold electrode [22].

The films produced electrochemically are expected to be more uniform and less porous than solution-cast films. However, they are also composed of small crystals, as shown for $(Ru(bpy)_3^{2+})(C_{60}^-)_2$ [23] and a mixed tetraphenylphosphonium fulleride bromide salt [24].

### 2.4. Other methods

In some studies, other techniques of $C_{60}$ immobilization were employed. For instance, a mixture containing ca. 60% of $C_{60}$ powder by volume and 40% of $LiClO_4$ containing polyethylene oxide, $(PEO)_8LiClO_4$, was successfully employed by Chabre et al. [26] in their studies on electrochemical intercalation of lithium into solid $C_{60}$. A vapor deposition technique seems to be particulary useful where uniformity of the film is important, e.g. for conductivity experiments [10]. Some preliminary results obtained in our laboratory suggest that $C_{60}$ could also be immobilized on a surface during the formation of self-assembled films onto a thiol-modified electrode [6].

## 3. General electrochemical behavior of the fullerene films

Because the oxidation of both solid [5, 6] and dissolved [1] $C_{60}$ usually results in irreversible multi-electron processes leading to a degradation of the $C_{60}$ molecule, most electrochemical studies of $C_{60}$ (and $C_{70}$) films are limited to the reduction processes; see, however, Refs. [4] and [27]. In general, the electrochemical behavior of $C_{60}$ films is rather complicated, as opposed to the well-defined consecutive one-electron reductions observed on the voltammograms of $C_{60}$ solutions [2]. Neither the background electrolyte anion nor the substrate electrode material appears to have a strong effect on the electrochemical behavior of the $C_{60}$ films. Most of the electrochemical studies on $C_{60}$ films employed acetonitrile (MeCN) as a solvent, not only because of the exceptionally low solubility of $C_{60}$ in MeCN but also because of its wide potential range. Unless otherwise stated, all the results described below have been obtained with MeCN as the solvent.

The main factor affecting the behavior of the fullerene films upon electroreduction is the nature of the cation of the background electrolyte, just as the structure, free energy, and solubility of the phases formed by electrochemical doping of $C_{60}$ with cations depend on the cation. The background electrolyte cations can be divided into two groups with respect to the CV behavior of the $C_{60}$ films in the potential range corresponding to the first reduction and reoxidation processes in MeCN. The first group of cations, hereafter referred to as the group of large cations, include tetrabutylammonium ($TBA^+$), tetrahexylammonium ($THA^+$), and tetraoctylammonium ($TOA^+$) cations. For reasons described below, we also include $Li^+$ in this group. For this group of cations, a large splitting is usually observed between the reduction and reoxidation processes of the film, as well as relatively stable CV behavior, which can be attained after a few initial scans. This stable electrochemical behavior frequently corresponds to a maximum electrochemical activity of the film and is hereafter referred to as the steady-state behavior. The second group of cations includes small alkaline metal and alkali earth metal cations as well as the tetraethylammonium ($TEA^+$) cation. The cathodic and anodic peak potentials are generally less widely spaced than for the cations belonging to the large-cation group, and the electrochemical activity of the film disappears after a few initial cycles. This group is hereafter called the small-cation group. The following two sections describe the general electrochemical behavior of the $C_{60}$ and ($C_{70}$) films in the presence of the background electrolytes belonging to these groups.

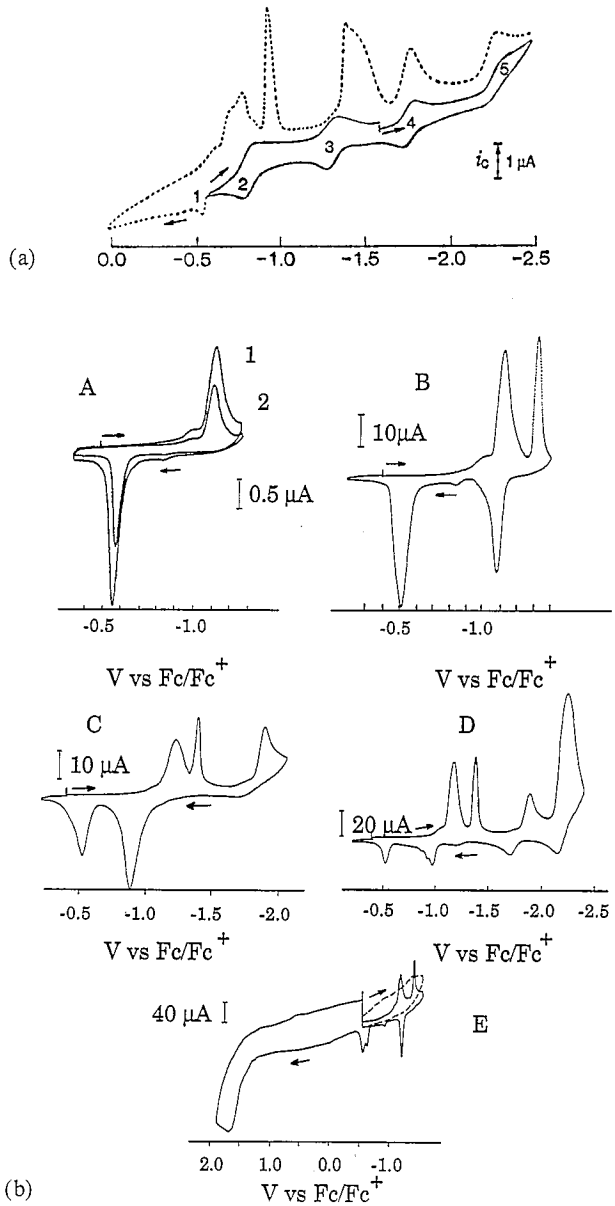


Fig. 2. (a) CV of ca. 0.45 mM $C_{60}^{3-}$ in MeCN, 0.1 M (TBA)$ClO_4$ at a 0.785 $mm^2$ Pt electrode, 0.1 V $s^{-1}$ scan rate, between −2.50 and −0.55 V (solid line) and between −2.5 and 0.0 V (dashed line). Reprinted with permission from Ref. [21]. Copyright 1992 American Chemical Society. (b) CV of $C_{60}$ films on a Pt electrode. (A, B) First and second reduction processes. Supporting electrolyte, 0.1 M (TBA)$AsF_6$; scan rate, (1) 0.2 and (2) 0.1 V $s^{-1}$; 250 μm-dia. electrode. (C) Third reduction. (D) Fourth reduction. (E) Oxidation reactions. Supporting electrolyte, 0.1 M $(TBA)_4$; scan rate, 0.2 V $s^{-1}$; 1 mm-dia electrode. Reprinted with permission from Ref. [6]. Copyright 1992 American Chemical Society.

### 3.1. Electrolytes with large cations

Up to five reduction peaks can be observed in the voltammograms of $C_{60}$ films in the presence of electrolytes containing $TBA^+$ [5, 6, 21] (Fig. 2), with the peak potentials roughly corresponding to those observed for the successive one-electron transfers to the dissolved $C_{60}$ [2]. Electrochemical quartz crystal mi-

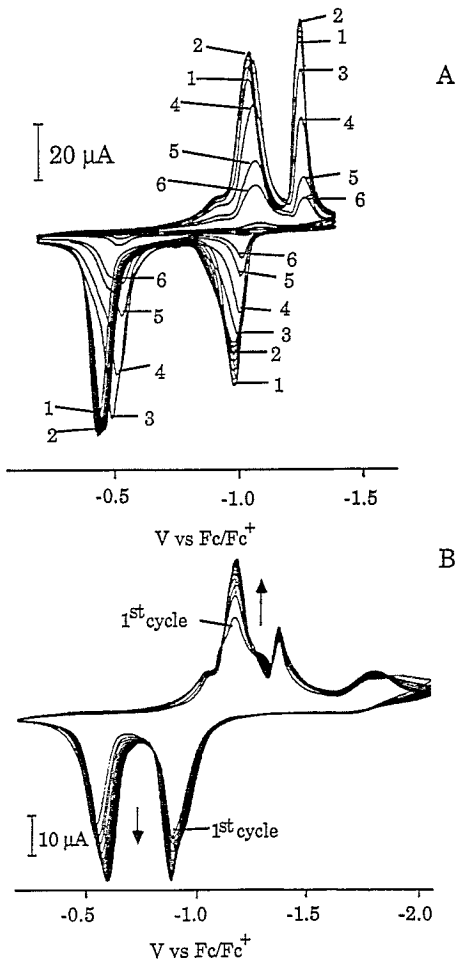


Fig. 3. Effect of continuous cycling of $C_{60}$ films on a 1 mm-dia. Pt electrode. Supporting electrolyte, 0.1 M (TBA)$AsF_6$; scan rate, 200 $mV^{-1}$ s. (A) Cycling over the first reduction process: 1, first cycle; 2, after 10 cycles; 3, after 5 min; 4, after 10 min; 5, after 20 min; 6, after 25 min. (B) Cycling over the third reduction process. Reprinted with permission from Ref. [6]. Copyright 1992 American Chemical Society.

crobalance (EQCM) experiments by Koh et al. [21], discussed in Section 4.1, showed that only the first three peaks are due to film reduction, whereas the two further cathodic peaks correspond to reduction of a dissolved $C_{60}^{3-}$ species. This finding explains why the shape and the peak potentials of the anodic scan are strongly influenced by the cathodic reversal potential (Fig. 2). Since the third reduction obviously corresponds to $C_{60}$ film dissolution, most studies of $C_{60}$ films were limited to the first two reduction/reoxidation processes.

A marked difference is usually observed between the first and subsequent scans during voltammetric experiments with drop-coated films [5, 6, 13, 14], irrespective of whether only the first or the first two reductions were studied. In some experiments [5, 6], smaller reduction and reoxidation charges were observed during the first scan than on subsequent ones, with no significant changes in either the peak potentials or peak shapes. Other researchers reported higher charges of the first scan [13, 14] and noticeably smaller reoxidation charges in the reverse scan. The first two reductions were said to occur simultaneously during the first voltammetric scan recorded for a relatively thick (equivalent to ~400 layers) $C_{60}$ film [13] but became resolved on subsequent scans. Similar behavior was observed by Nishizawa et al. [10] for compact vapor-deposited films and by Koh et al. [22] for electrochemically grown films. These findings suggest that the preparation method and the initial film structure affect the initial electrochemical behavior of the film. For solution-cast films, entrapped casting solvent appears to play a role in determining the initial electrochemical behavior of the film [6] (see, also, Section 4 below). Some electrochemically grown films may initially contain trapped background electrolyte [22]. The entrapped casting solvents are said to be released during the first few scans [6, 14]. After continuous potential cycling over the first or first two reduction and reoxidation processes, a relatively stable (steady-state) voltammetric behavior can be attained. In the steady state, the peak potentials do not change and reduction and reoxidation charges are identical within experimental error. In fact, they do decrease slightly from cycle to cycle, and after a very long time of potential cycling, the electrochemical activity of the film is suppressed completely [5, 6, 14] (Fig. 3). There is no agreement as to why the long-time potential cycling leads to a gradual loss of electrochemical activity of the film. Jehoulet et al. [6] reported the presence of a resistive film on the electrode after the $C_{60}$ lost its activity while, according to Tatsuma et al. [14], the loss of activity is due to the complete dissolution of the film; some dissolution of the film seems possible (see Sections 4 and 5). The small cathodic and anodic prewaves that are seen on the steady-state voltammograms of the $C_{60}$ film (Fig. 3) are also believed to originate from partial film dissolution (see Section 4). The differences in the long-time electrochemical behavior reported by the two research teams may be due to the presence of some impurities in the solvents or electrolytes. Even trace amounts of contaminants can affect the long-time electrochemical behavior of the film, since very small amounts of $C_{60}$, usually in the nanomolar range, are used for film preparation.

The steady-state voltammograms for $C_{60}$ films reported in the literature are very similar, regardless of the different methods of preparation and the different initial electrochemical behavior observed [5, 6, 10, 13, 14]. The peak currents for both reductions and oxidations have been found to be proportional to the scan rate up to 0.2 V $s^{-1}$ [5, 6, 10, 12, 14], as expected for a surface-confined species. However, the peak widths at half-height are smaller than expected (91 mV [28]) for the surface peaks [5, 6, 12]. A lack of dependence of the

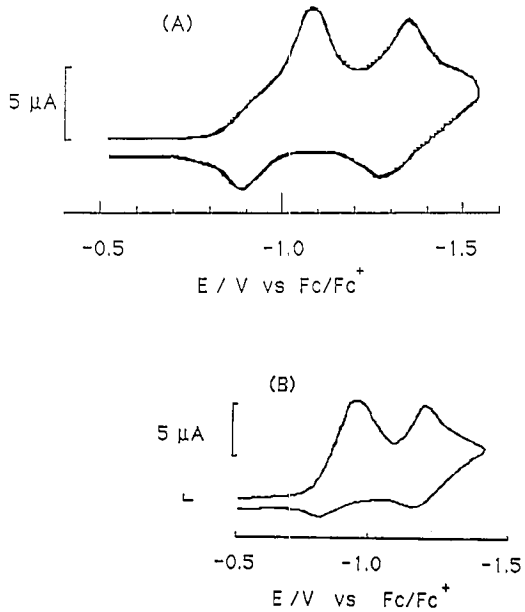


Fig. 4. CV of LB films of $C_{60}$ on a hydrophobic Au electrode in a 0.1 M (TBA)$BF_4$/MeCN solution. Pure $C_{60}$ solution film transferred vertically. (A) 50μl of $10^{-4}$ M $C_{60}$ at $\pi = 5\,mN^{-1}\,m$ ($\pi$, surface pressure) (B) 1:1 mixture of $C_{60}$:AA, $\pi = 5\,mN\,m^{-1}$; scan rate $= 0.2\,V\,s^{-1}$. Reprinted with permission from Ref. [19]. Copyright 1993 American Chemical Society.

peak potentials on the scan rate applied was reported by Compton et al. [12]. Our results [6] indicated that the cathodic peak potentials were essentially constant while the anodic ones moves slightly toward less negative potentials on increasing the scan rate. Quantitative coulometry performed with the solution-cast films revealed that the charge injected during the first reduction of the thin films (average film thickness equivalent to 40 layers or less) corresponded to the complete one-electron reduction of the film [5, 6, 13] and therefore to the formation of the ($TBA^+$) ($C_{60}^-$) phase. The charge corresponding to the second reduction/reoxidation process was, however, systematically lower than expected for injection of another electron per $C_{60}$ molecule. It was usually close to 50% of the charge associated with the first pair of reduction/reoxidation peaks [5, 6, 13]. On the other hand, the EQCM studies performed with the electrochemically grown $C_{60}$ films [21, 22] suggest that the phase that is being formed in the second reduction step is ($TBA^+$)$_2$($C_{60}^{2-}$). The reason for this discrepancy is unclear. Some differences in structure of the solution-cast and electrochemically grown films seem likely.

Voltammograms of LB films of both pure $C_{60}$ and its mixtures with arachidic acid [6, 19] exhibit, as a rule, much smaller peak splittings for both reduction/reoxidation processes (Fig. 4) than those observed for generally thicker films obtained using the other preparation techniques, in line with the smaller reorganization expected for the thinner films upon reduction (see below). Partial overlapping of both reduction and reoxidation processes (Fig. 4) makes comparison of the charges corresponding to the subsequent electrode reactions difficult. However, as can be seen from Fig. 4, the reoxidation charge is significantly smaller than the reduction charge, indicating irreversible film damage due to either dissolution or chemical inactivation.

Very interesting behavior has been reported recently [20] for the LB films of 1-tert-butyl-1,9-dihydrofullerene-60 in an MeCN solution of (TBA)$PF_6$. Voltammograms of the monolayer of that compound exhibited three well-defined peaks corresponding to the consecutive one-electron-transfer reactions. The peak splittings of the first two waves were 65–70 mV and, suprisingly, the peak currents varied with the square root of scan rate, which is characteristic of diffusion control. This behavior persisted even at scan rates as low as $1.0\,mV\,s^{-1}$. When there were more than three monolayers of the compound on the electrode surface, the voltammograms were severely distorted. The authors suggested that hindered ion transport into the film is responsible for the atypical behavior observed.

For background electrolytes containing $THA^+$ or $TOA^+$ cations, conflicting results have been reported. According to Jehoulet et al. [5, 6], stable voltammetric behavior of the solution-cast films could be observed

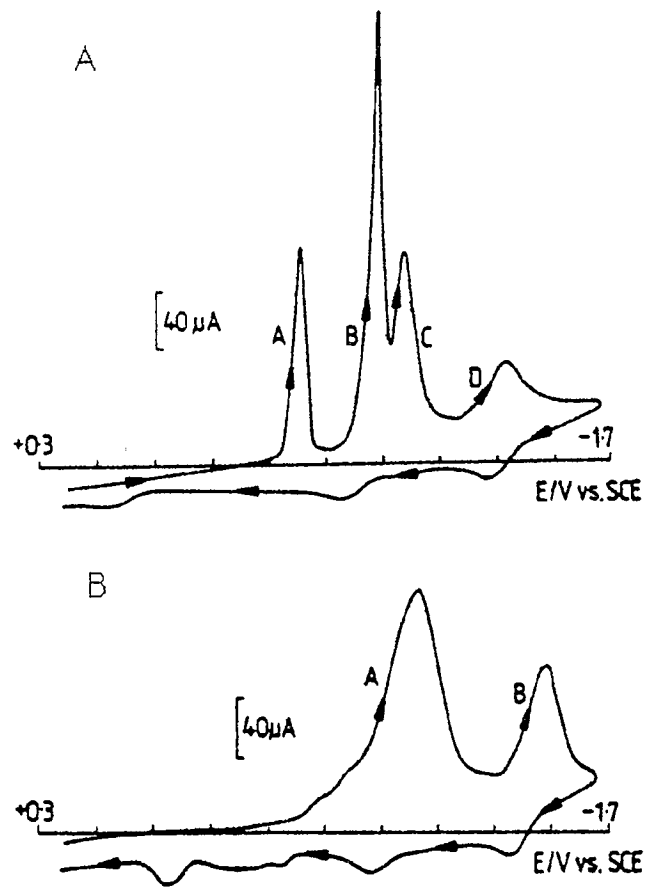


Fig. 5(a)

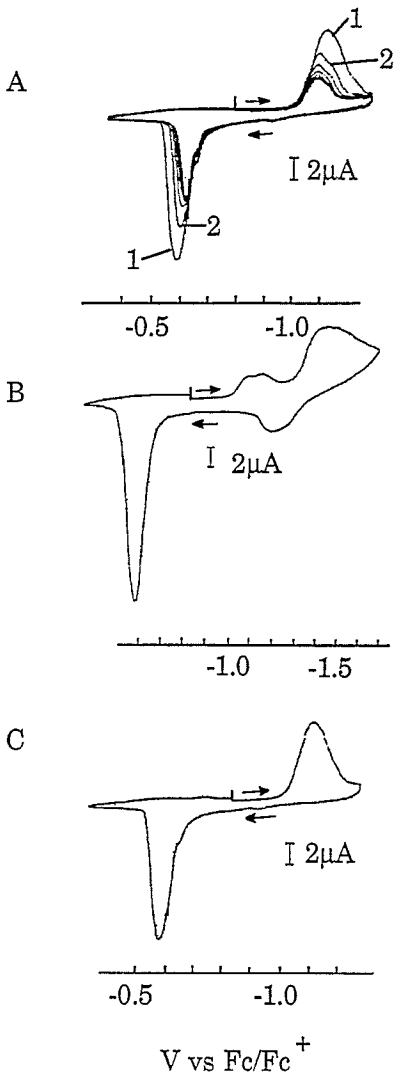


(b)

Fig. 5. (a) CV of a thin-layer $C_{60}$ film in 0.1 M (A) tetra-n-hexylammonium perchlorate (THAP) and (B) tetra-n-octylammonium perchlorate (TOAP) supporting electrolyte/MeCN; scan rate, 0.1 V $s^{-1}$, 0.4 $cm^2$ Au or Pt electrode. Reprinted with permission from Ref. [13]. Copyright 1993 Elsevier. (b) CV of a $C_{60}$ film in 0.1 M (TOA)$AsF_6$; scan rate, 0.2 V $s^{-1}$; 250 μm-dia. Pt electrode. (A) Continuous cycling; (B) second reduction; (C) first reduction. Reprinted with permission from Ref. [6]. Copyright 1992 American Chemical Society.

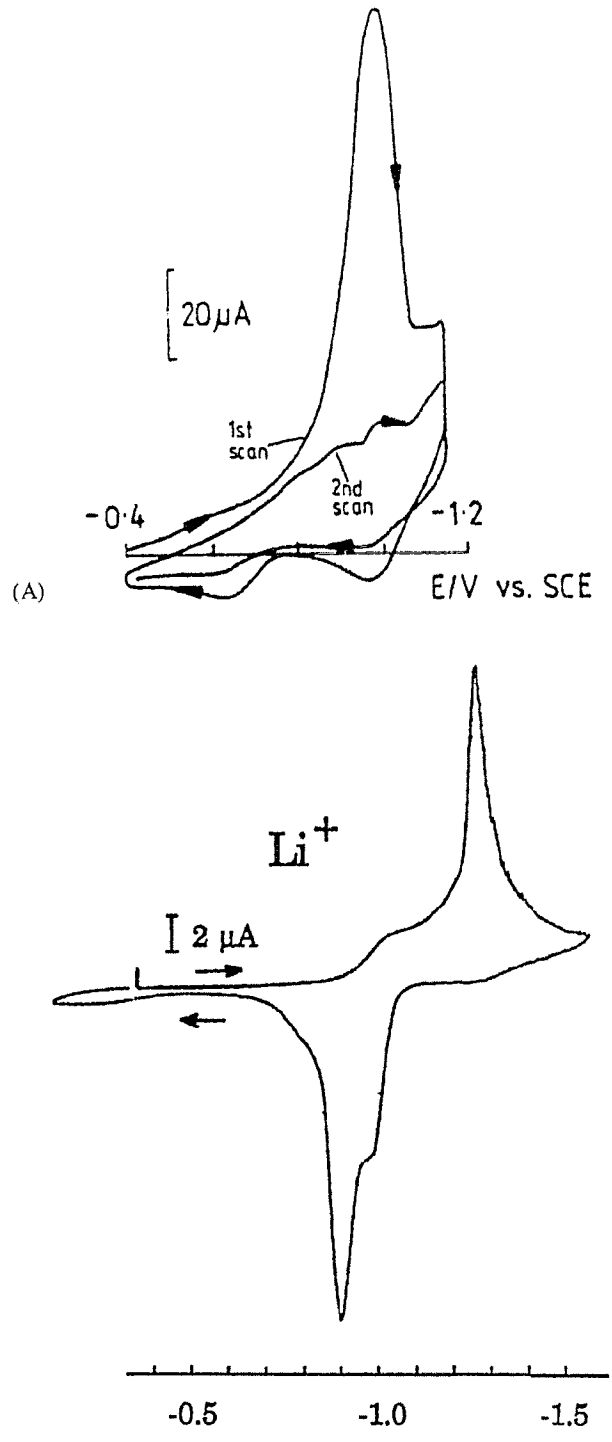


(A)

(B)

Fig. 6. (A) CV showing the reduction of a $C_{60}$ film in 0.1 M $LiClO_4$ at 0.1 V $s^{-1}$. Reprinted with permission from Ref. [13]. Copyright 1993 Elsevier. (B) CV of a $C_{60}$ film in 0.1 M $LiAsF_6$ with a 250 μm-dia. Au electrode at 200 mV $s^{-1}$. Reprinted with permission from Ref. [6]. Copyright 1992 American Chemical Society.

with these electrolytes, while Compton et al. [13] reported a significant loss of electrochemical activity of the film after the first reduction/reoxidation cycle. The voltammograms obtained in the two laboratories had markedly different shapes (Fig. 5). The discrepancy of the results cannot be attributed to different anions of the background electrolytes employed, which were perchlorates [13] and hexafluoroarsenates [5, 6]. More probable seems to be the presence of traces of water in the solutions studied by Compton et al. [13]. This supposition is based on the fact that the experiments described in Refs. [5] and [6] were performed in a dry-box with "water-free" Burdick & Jackson MeCN, which, as we knew from our other studies [29], contained less than $10^{-5}$ M water. The water content in the solutions studied by Compton et al. apparently was not controlled. In light of the above considerations, the number of electrons involved in the $C_{60}$ film reductions (two for each $C_{60}$ molecule for the first reduction peak

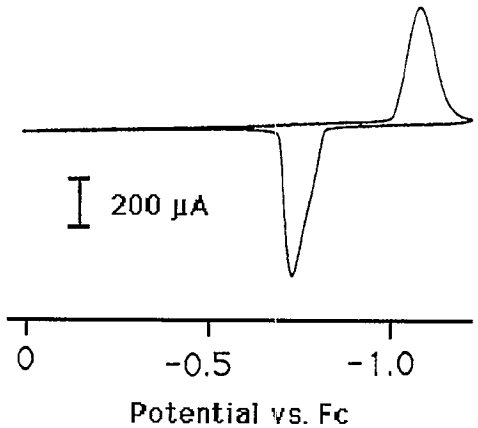


Fig. 7. Steady-state voltammogram of a $C_{60}$ film (16.6 nmol) at 50 mV $s^{-1}$ in 0.05 M $Cd(bpy)_3(PF_6)_2$. Fc, ferrocene.

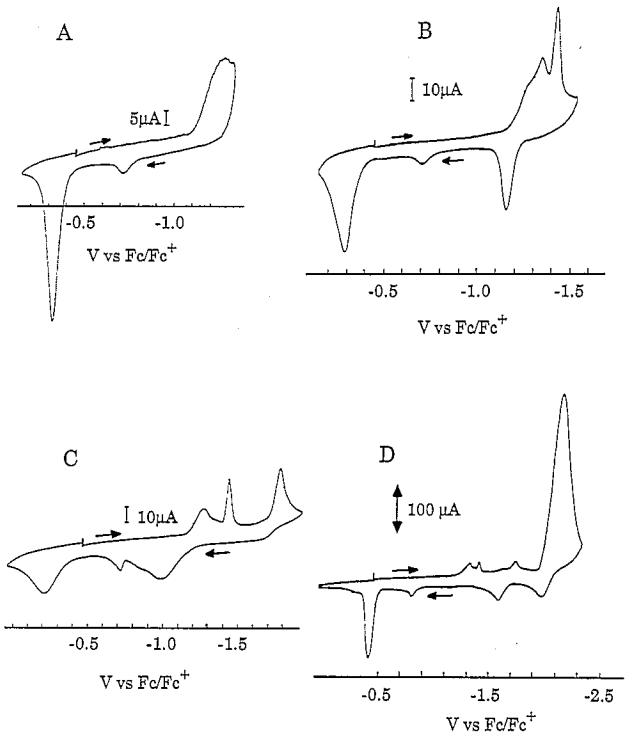


Fig. 8. CV of $C_{70}$ films on a 2 mm-dia. Au electrode. Reduction reactions on the film: A, scan over first reduction peak; B, over second reduction; C, over third reduction; D, over fourth reduction. Supporting electrolyte, 0.1 M $(TBA)BF_4$; scan rate, 200 mV $s^{-1}$. Reprinted with permission from Ref. [6]. Copyright 1992 American Chemical Society.

and 0.5 for the second reduction in the $(TOA)ClO_4$ solution; and two for the first, 0.5–1.0 for the second and third, and $\approx$0.5 for the fourth reduction in the $(THA)ClO_4$ solution) that were determined by Compton et al. [13] probably can be attributed to follow-up reactions. Generally, the electrochemistry of $C_{60}$ films in the presence of $(THA)AsF_6$ and $(TOA)AsF_6$ [5, 6] is similar to their electrochemistry in the presence of $TBA^+$ salts (Fig. 5). However, there were some differences in the electrochemical behavior compared to that of $TBA^+$. In $(TOA)AsF_6$ solution, if the potential was continuously scanned over the first pair of waves, the peak currents decreased to a steady-state value within 5–10 min (Fig. 5), and the second reduction and reoxidation peaks were much broader. Charges calculated from integration of the CV waves showed that the second reduction involved approximately 1.5 times more charge relative to the first wave. Discrepancies similar to those reported for the $THA^+$ and $TOA^+$ solutions were also found with electrolytes containing $Li^+$ [6, 13] (Fig. 6). The same effects of trace water may apply. The reason $Li^+$ is placed in the group of large cations is that the voltammetric behavior of the $C_{60}$ films in water-free $LiAsF_6$ solutions [6], i.e. relatively large peak splitting and almost 100% efficiency of the reoxidation process (Fig. 6), more closely resembles the behavior observed in the presence of $TBA^+$ salts than the behavior characteristic for the alkali metal and alkaline earth metal salts (Section 3.2).

Some other solvents have also been used to study Li intercalation into the $C_{60}$ phase. Unstable electrochemical behavior was reported for solution-cast films of $C_{60}$ in a propylene carbonate solution of $LiClO_4$ [15]. This was attributed to dissolution effects. Reversible multistep lithium intercalation into solid $C_{60}$ at 80 °C was observed by Chabre et al. [26], who used solid polyethylene oxide/$LiClO_4$ as a background electrolyte. The peak-to-peak separation for the first intercalation (reduction/reoxidation) step was around 200 mV. This step corresponded to formation of a $Li_{0.5}C_{60}$ phase.

Our recent studies [30] show that very stable and well-defined CV behavior of the $C_{60}$ films in MeCN can be observed in solutions of metal bipyridine complex salts [$M(bpy)_3^{2+}$, M = Ni, Cd, Fe] (Fig. 7).

The voltammetric behavior of $C_{70}$ films has been studied to a lesser extent than $C_{60}$; in a $(TBA)BF_4$ solution [6], the CV is generally similar to the behavior of the $C_{60}$ films in $TBA^+$ solutions (Fig. 8). The peak splitting for the first reduction/reoxidation process was somewhat larger than for the $C_{60}$ films, while it was similar for the second reduction/reoxidation process. The effect of continuous scanning was different from that observed with the $C_{60}$ films (Fig. 9). Only about 25% of the material was reduced during the first scan, assuming a one-electron transfer. Upon continuous scanning over the first or the first two reduction and reoxidation peaks, the peaks continued to grow until about 31% of the material was reduced. Upon further reduction, the peak currents started to decrease and the reoxidation charges became lower than the reduction ones. Electrochemical activity of the film was suppressed after a longer time than for the $C_{60}$ films studied under comparable conditions [6]. A more complicated behavior was observed upon continuous cy-

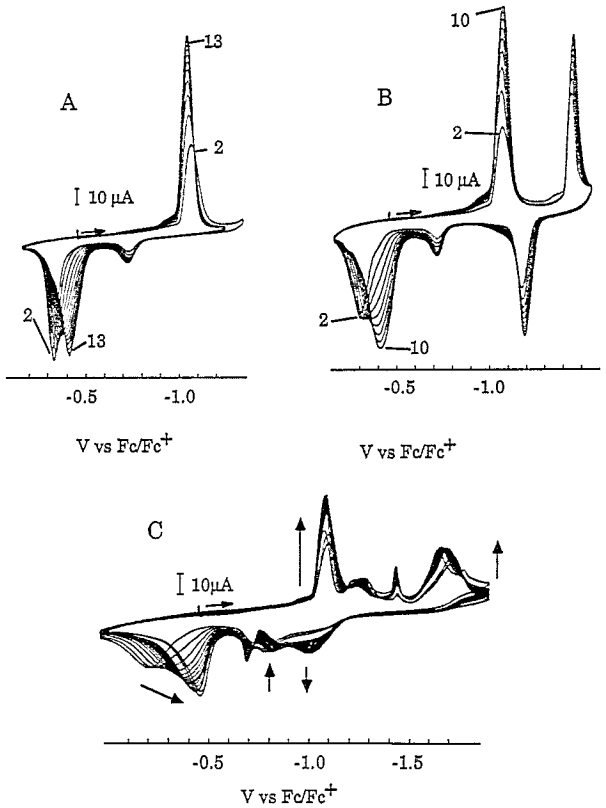


Fig. 9. Effect of continuous cycling of $C_{70}$ films on a 2 mm-dia. Au electrode. Supporting electrolyte, 0.1 M $(TBA)BF_4$; scan rate, 200 mV $s^{-1}$. (A) Over first reduction wave; (B) over second reduction; (C) over third reduction. Numbers indicate cycle number and arrows indicate peak behavior with time. Reprinted with permission from Ref. [6]. Copyright 1992 American Chemical Society.

cling extended to the third reduction wave. The products of the fourth reduction wave were found to be unstable.

### 3.2. Electrolytes with small cations

Very unstable voltammetric behavior, usually limited to a few initial scans, was observed for the $C_{60}$ films in MeCN solutions of $Na^+$ [5, 6, 13, 14], $K^+$ [5, 6], $Cs^+$ [5, 6], $Ba^{2+}$ [13], and $TEA^+$ [6, 13] salts. The same was true for $C_{70}$ films in a $KPF_6$ solution [6], although in that case, stability was increased with respect to that observed for the $C_{60}$ films. Multiple reduction peaks, frequently merging in a large cathodic wave, as well as two small anodic peaks can be seen on the voltammograms recorded for these background electrolytes (Fig. 10). The number of electrons transferred during the reduction processes contributing to the large cathodic waves was found to be identical for all of the cations and equals one electron per $C_{60}$ molecule [6, 13], except for $TEA^+$, for which a number close to one was reported by us [6] and two electrons were determined by Compton et al. [13]. There is no certainty as to the cause of the deactivation of the films in these

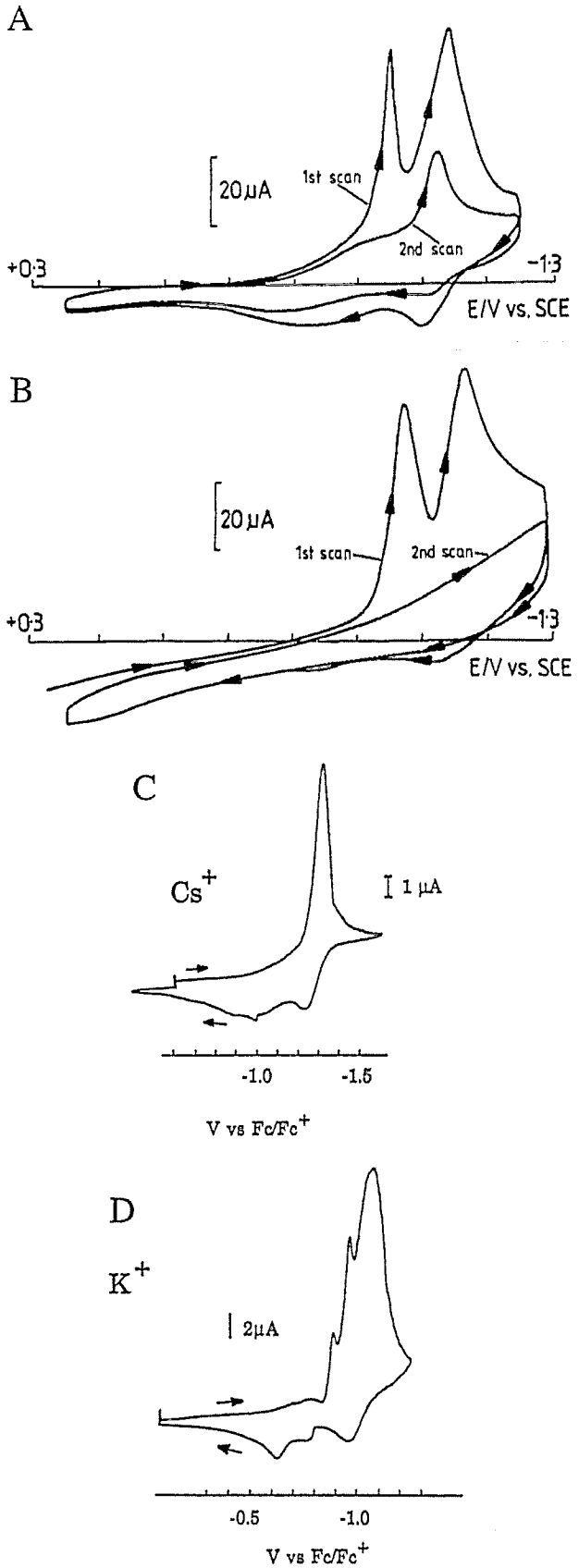


Fig. 10. CVs of $C_{60}$ films in 0.1 M electrolyte. At 100 mV $s^{-1}$: (A) $Ba(ClO_4)_2$; (B) $NaClO_4$. At 200 mV$s^{-1}$: (C) $CsAsF_6$; (D) $KPF_6$. (A, B) Reprinted with permission from Ref. [13]. Copyright 1993 Elsevier. (C, D) Reprinted with permission from Ref. [6]. Copyright 1992 American Chemical Society.

electrolytes. Both research teams detected a resistive film on the electrode surface after the original film lost its electrochemical activity. On the other hand, some of the EQCM studies (see Section 4, below) point to film dissolution.

## 4. $C_{60}$ film studies using other analytical techniques

Because of the complex nature of the electrochemistry of $C_{60}$ films, various additional analytical techniques have been applied to this system to further our understanding of the chemical processes involved. These techniques include use of the electrochemical quartz crystal microbalance (EQCM), the scanning electrochemical microscope (SECM), laser-desorption mass spectroscopy (LDMS), and surface-enhanced Raman spectroscopy (SERS). Each provides additional insight into the nature of the film during reduction and oxidation processes.

### *4.1. Electrochemical quartz crystal microbalance (EQCM) studies*

The Kadish, Bard, and Oyama research groups have all applied the EQCM to the study of fullerene films [7, 14, 21, 22]. The EQCM technique has matured in recent years to include the study of many types of complex thin films. Several reviews [31] of this area appear in the literature, so only a brief mention of the applicable principles involved will be made here. The EQCM is sensitive to viscosity and mass changes on a thin metal electrode on a piezoelectric quartz crystal. Quantitatively, this mass sensitivity takes the form of the Sauerbray equation, $\Delta f = -C_f(\Delta m/A)$, where $f$ is the frequency, $m$ is the mass, $A$ is the area, and $C_f$ is a constant for a given design. The frequency of the crystal decreases as mass on the electrode surface increases. However, this assumes no shearing forces are caused by the film (i.e. that the film is thin, rigid, and smooth). In all EQCM/$C_{60}$ film research to date, the frequency data were taken as representing mass effects only, and shearing force contributions have been neglected, despite the knowledge that the films are commonly made of small crystallites. In many cases, such as dissolution, this approach is an acceptable practice. It becomes more questionable whether or not a frequency is altered by a change in film shearing forces when structural reorganization within a film occurs (as with $TBA^+$, for example). The dissolution and redeposition of the film indicated by light microscopy and SECM (Section 4.2) for $TBA^+$ might be expected to cause a frequency shift of its own, since some crystallites dissolve completely and others grow. No impedance analysis has been done with $C_{60}$ films to confirm what part of the frequency response may be the result of shearing changes.

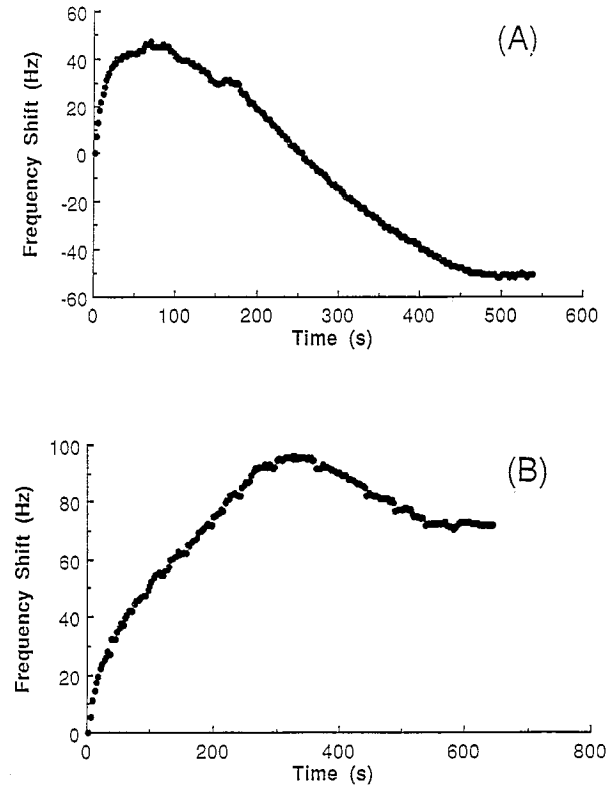


Fig. 11. Frequency shift vs. time for two 4.3 μg $C_{60}$ films after applying potentials of (A) −0.75 and (B) −1.00 V vs. silver quasi-reference electrode (AgQRE). Reprinted with permission from Ref. [7]. Copyright 1992 American Chemical Society.

Nevertheless, it is clear that EQCM has contributed much toward the understanding of $C_{60}$ films. The first two EQCM studies concentrated solely on the $TBA^+$/$C_{60}$ system, but took two different approaches. One approach started with a neutral film cast on the EQCM electrode [7], while the other started with a solution of the soluble $C_{60}^{3-}$ formed from the electrolysis of a slurry of $C_{60}$ in MeCN [21]. The EQCM result of two potential step experiments starting with a $C_{60}$ film are shown in Fig. 11 [7]. During a step past the first reduction potential with a fresh film, an initial mass loss (frequency increase) occurs for the first 2 min, followed by an even greater mass gain (frequency decrease). Quantitative analysis of these results indicated that about a quarter of the film dissolves, while three-quarters of the film becomes doped with $TBA^+$. A step past the second reduction potential with a fresh film shows an initial mass loss, indicating that dissolution dominates the first 6 min, with a much smaller contribution from cation incorporation. In this case, qualitative calculations show about 43% of the film dissolves with the balance of the film being doped with two $TBA^+$ cations per $C_{60}$. An EQCM CV of the film at 200 mV $s^{-1}$ shows a large mass increase at the $C_{60}/C_{60}^-$ reduction wave and competing dissolution and cation incorporation at the $C_{60}^-/C_{60}^{2-}$ reduction wave. At this scan rate, no

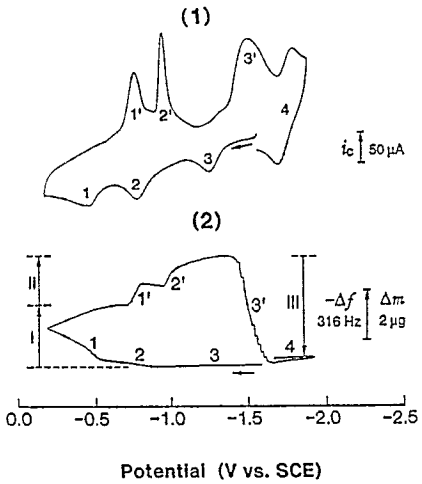


Fig. 12. Simultaneous CV (curve 1) and EQCM frequency response (curve 2) of ca. 0.63 mM $C_{60}^{3-}$ in MeCN, 0.1 M $(TBA)ClO_4$ at a Au/quartz electrode; scan rate, 0.1 V $s^{-1}$. The overall mass changes given by the Roman numerals correspond to (I) deposition of the neutral $C_{60}$ film, (II) the stepwise uptake of $TBA^+$ into the reduced film, and (III) the electrodissolution of the $(TBA^+)_2(C_{60}^{2-})$ film. Reprinted with permission from Ref. [21]. Copyright 1992 American Chemical Society.

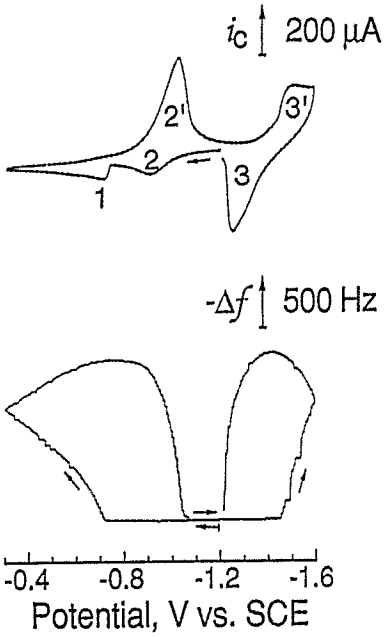


Fig. 13. Simultaneous CV and microgravimetry with EQCM at a Au/quartz electrode of ca. 1.30 mM $C_{60}^{2-}$ in 0.1 M $CsAsF_6$ MeCN; scan rate, 0.1 V $s^{-1}$. Reprinted with permission from Ref. [22]. Copyright 1993 American Chemical Society.

mass changes are indicated upon the reverse oxidation waves. Initially, $TBA^+$ was thought to be trapped with no counter charge balance in the film, but further studies [14, 22] showed that this behavior is really cation expulsion and anion incorporation within the film. At this scan rate, the two processes happen to roughly balance each other. Similar results were obtained by Koh et al. [21], who recorded the EQCM CVs at 100 mV $s^{-1}$ starting with $C_{60}^{3-}$ (Fig. 12). Oxidation to $C_{60}^-$ produced only a very small mass increase, indicating solubility of $C_{60}^-$. Further oxidation to neutral $C_{60}$ resulted in a large mass gain. This film, when reduced back to $C_{60}^-$ and $C_{60}^{2-}$, showed a mass increase similar to the result obtained by Zhou et al. [7]. Reduction of the film to $C_{60}^{3-}$ resulted in total dissolution of the film, and the $C_{60}^{3-}/C_{60}^{4-}$ reduction wave was shown to be a solution couple.

EQCM studies were continued by Koh et al. [22], starting with solutions of $C_{60}^{2-}$ or $C_{60}^{3-}$ and MeCN in different supporting electrolytes. These authors found that the films adhered much better to a nonpolished surface of a Au/quartz crystal than to a mirror-finished one. Both earlier EQCM studies [7, 21] had used nonpolished electrode surfaces. This suggests that some film loss may be a function of the roughness of the gold substrate. They also reported that much better resolution of the CV current peaks could be observed by scanning at slower rates than those used in previous studies (20 or 50 mV $s^{-1}$ vs. 200 or 100 mV $s^{-1}$). With $KPF_6$, only a mass increase was seen upon oxidation of the initial $C_{60}^{2-}$ solution to the neutral $C_{60}$, and an equal mass loss was observed upon the reduction of this neutral film. Thus, $C_{60}^-$, $C_{60}^{2-}$, and $C_{60}^{3-}$ are all soluble at the millimolar level in MeCN in the presence of $KPF_6$ electrolyte. With $CsAsF_6$ electrolyte, the only significant difference was the precipitation of $Cs_3C_{60}$ upon reduction to $C_{60}^{3-}$. Thus, $C_{60}^-$ and $C_{60}^{2-}$ were soluble, but $C_{60}^{3-}$ and neutral $C_{60}$ were insoluble (Fig. 13). With $Ca(PF_6)_2$, $C_{60}^{2-}$ and $C_{60}^{3-}$ were soluble, while $C_{60}^-$ slowly precipitated out of solution forming a $Ca(C_{60})_2$ film. Finally, in a reexamination of the $TBA^+$ system, they found that, at high scan rates (>0.1 V $s^{-1}$) and starting with a $C_{60}^{3-}$ solution, the $C_{60}^{3-}/C_{60}^{2-}$ and $C_{60}^{2-}/C_{60}^-$ oxidations only behave as solution couples, but at lower scan rates (<0.02 V $s^{-1}$), mass increases are observed for these oxidations forming $(TBA)_2C_{60}$ and $(TBA)C_{60}$ films. Further evidence of entrapment of the $(TBA)ClO_4$ electrolyte was obtained by studying the neutral film grown at fast and slow scan rates using CV–EQCM (Fig. 14). Slowly grown films resemble solution-cast films in the EQCM response, i.e. a mass increase upon reduction, while rapidly grown films show a large mass decrease upon reduction, indicating increased solubility of $C_{60}$ anions, perchlorate expulsion from the film, or both.

Tatsuma et al. [14] studied solution-cast $C_{60}$ films in the presence of $Na^+$, $Li^+$, and $TBA^+$. They used only a very slow scan rate (10 mV $s^{-1}$) in their CV–EQCM studies. The $TBA^+$ results were similar to those obtained with slowly grown films [22]. Eventual loss of film activity after 20 cycles over the first and second reductions was shown to be the result of film dissolution. $C_{60}^{3-}$ was shown to be completely soluble, in

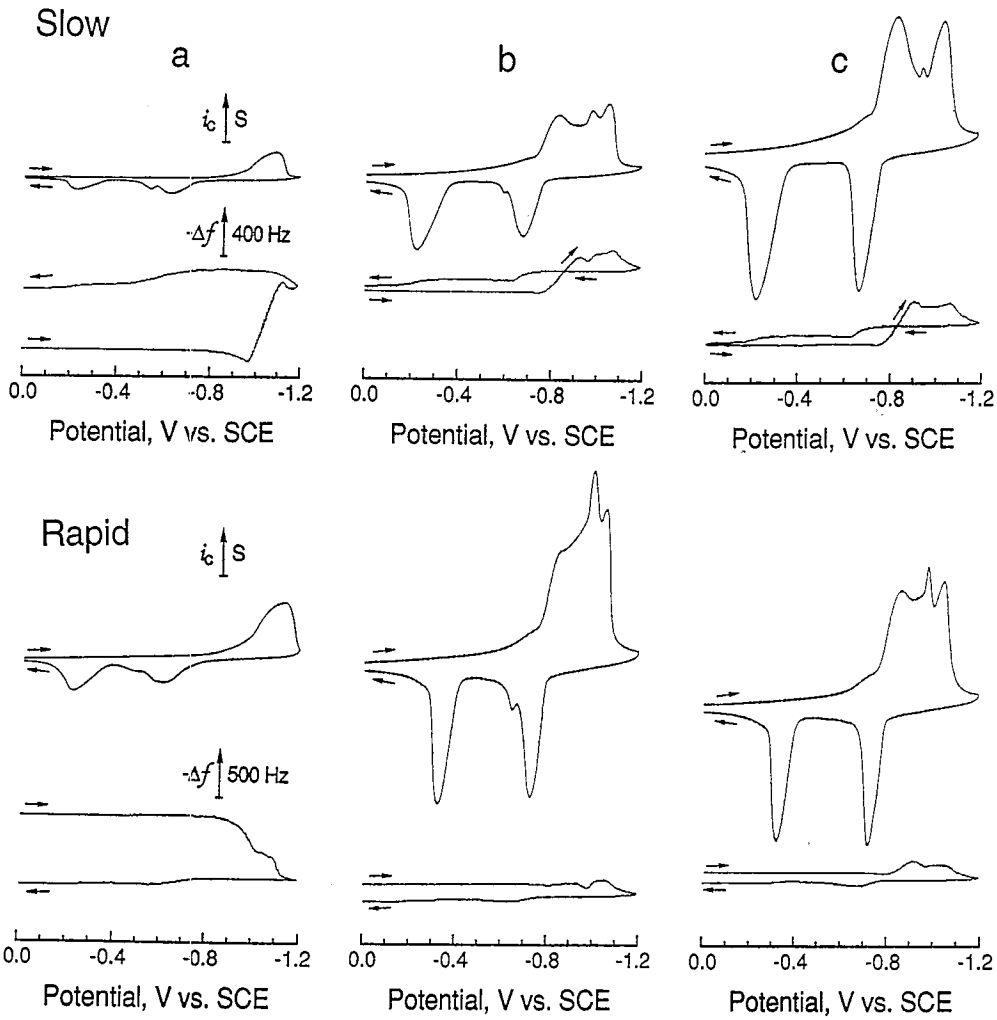


Fig. 14. Comparison of slow and rapid electrochemical film growth using EQCM of a $C_{60}$ film grown on a Au/quartz electrode in 0.1 M (TBA)$ClO_4$/MeCN at 0.1 V $s^{-1}$. The slow film was electrodeposited at 0.0 V for 6.5 min from ca. 0.09 mN $C_{60}^{3-}$ in 0.1 M (TBA)$ClO_4$/MeCN, while the rapid film took 3.0 min from ca. 0.3 mM $C_{60}^{3-}$. (a) First cycles; (b) second cycles; (c) third cycles. Current scale for slow films: (a) 2.0, (b) 0.40, and (c) 0.20 mA. Current scale for rapid films: (a) 1.0, (b) and (c) 0.10 mA. Reprinted with permission from Ref. [22]. Copyright 1993 American Chemical Society.

accord with earlier studies [21, 22]. The first cycle was anion-dependent, with (TBA)$PF_6$ producing a mass loss not present with (TBA)$ClO_4$ when the scan direction was reversed from negative to positive. $Na^+$ and $Li^+$ favored the dissolution of the film, as seen earlier with $K^+$ [22].

Our group has continued CV–EQCM work with metal complex cation electrolytes using solution-cast films [30]. This work shows that for the electrolytes $M(bpy)_3(PF_6)_2$, where M = Ni, Cd, or Fe and bpy is bipyridine, the first reduction of the film is completely charge-balanced by cation incorporation (Fig. 15). Reoxidation of the film involves an initial mass increase (anion incorporation) followed by a larger mass decrease, implying cation expulsion from the film. A net mass increase is observed upon cycling, indicating that the electrolyte (both anion and cation) becomes trapped within the film.

### 4.2. Scanning electrochemical microscopy (SECM)

Although SECM has been applied to many other complex film systems and the area has been extensively reviewed [32], only one SECM study has been performed in the area of $C_{60}$ films [6]. This study, however, predated the EQCM work and looked only at the first $C_{60}/C_{60}^-$ reduction in the presence of $TBA^+$. Three separate experiments were performed utilizing three different applications of the SECM. In SECM, the change in the steady-state current of a mediator at a microelectrode tip near a substrate is recorded as the tip is moved. Over a nonconductive substrate, diffusion is blocked by the substrate, thereby reducing the steady-state current as the tip approaches the substrate (negative feedback). Over a conductive substrate, the mediator is regenerated at the substrate, and the steady-state current is increased (positive feedback).

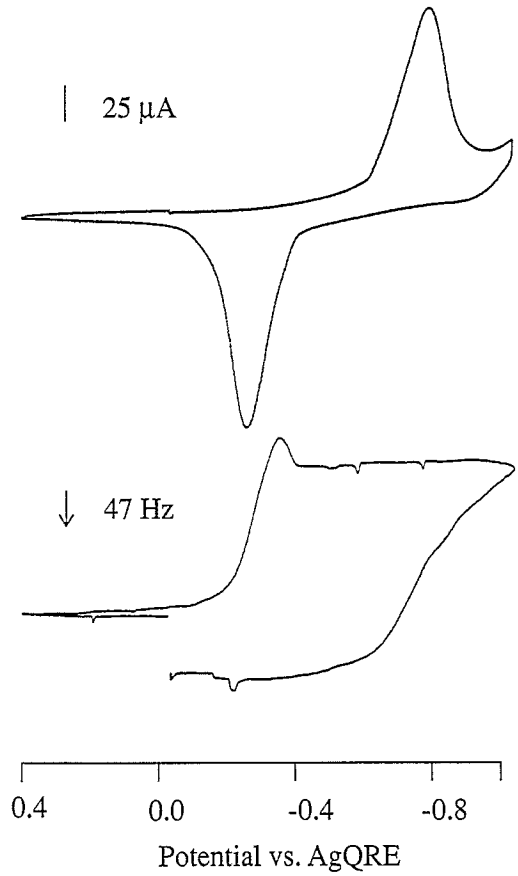


Fig. 15. CV and EQCM frequency response for 9 μg $C_{60}$ in 45 mM $Zn(bpy)_3(PF_6)_2$/MeCN electrolyte; 5 MHz Au/quartz electrode. Arrow indicates increasing frequency (decreasing mass).

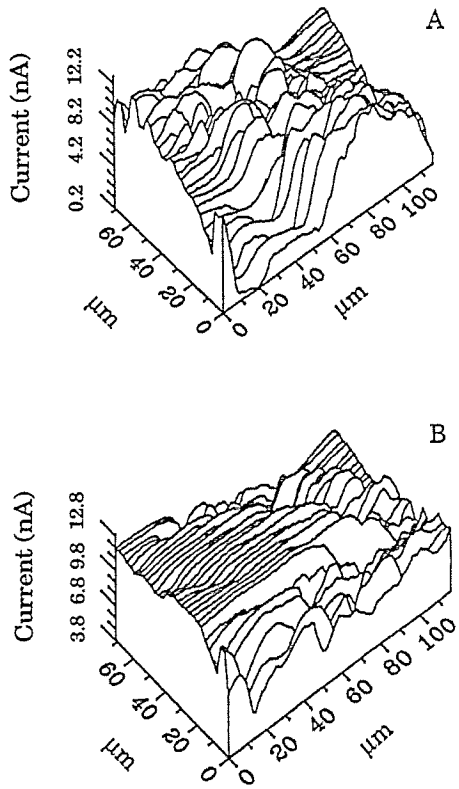


Fig. 16. SECM image of a $C_{60}$ film on a Au electrode at open circuit before any electrochemical experiments at two different locations. Solution, MeCN containing 0.1 M(TBA)$BF_4$ and 5.8 mM TMPD; tip, 5 μm-dia. Pt; $i_{T,\infty} = 11.8$ nA. Reprinted with permission from Ref. [6]. Copyright 1992 American Chemical Society.

The first experiment used a small tip with a tetramethyl-*p*-phenylenediamine (TMPD) mediator to image the morphology of the solution-cast $C_{60}$ film (Fig. 16). In most cases, the steady-state tip current near the film was smaller than the steady-state tip current far away from the film, indicating that the $TMPD^+$ was not reduced at the film and it was not conductive. Some areas of the filmed electrode showed positive feedback behavior, indicating a greater porosity of the film as more of the conductive gold substrate was exposed to regenerate the TMPD. The film was shown to be very non-uniform with some areas of high porosity and others with little porosity.

A second experiment used the current feedback mode as a small tip approached a $C_{60}$ film substrate to determine the in-situ conductivity of neutral, partially reduced, and fully reduced films with (TBA)$BF_4$ electrolyte. The steady-state oxidation current of a TMPD mediator was used to determine the type of feedback experienced by the tip approaching a fullerene film at the edge of a platinum disk sealed in Teflon (Fig. 17). The neutral and fully reduced films showed only a small positive feedback resulting from film porosity and a sharp conductivity decrease at parts of the film over the Teflon. The positive feedback current was larger for the partially reduced film, indicating greater conductivity. Moreover, the conductivity of the partially reduced film was more uniform, and positive feedback was observed over the Teflon substrate region. This indicated that the higher feedback current was not caused by an increase in porosity, but an increase in the conductivity of the film, which allowed for electron transfer from the platinum to more of the film, including areas of the film over the Teflon substrate. These results are similar to those later published by Nishizawa et al. [10] which showed improved conductivity with partially reduced films using a different technique.

Finally, the SECM was used in a substrate generation/tip collection mode to investigate the solubility of the reduced $C_{60}^-$ film in the presence of $TBA^+$. The substrate with the film was scanned over the first reduction and oxidation waves, and the smaller tip was held at a potential to monitor the amount of $C_{60}^-$ in the solution close to the substrate. The tip current of the initial scan was significant, showing dissolution of $C_{60}^-$ into solution, but dissolution was reduced in later cycles (Fig. 18). Overall, the substrate current decreased only slightly aften ten potential cycles.

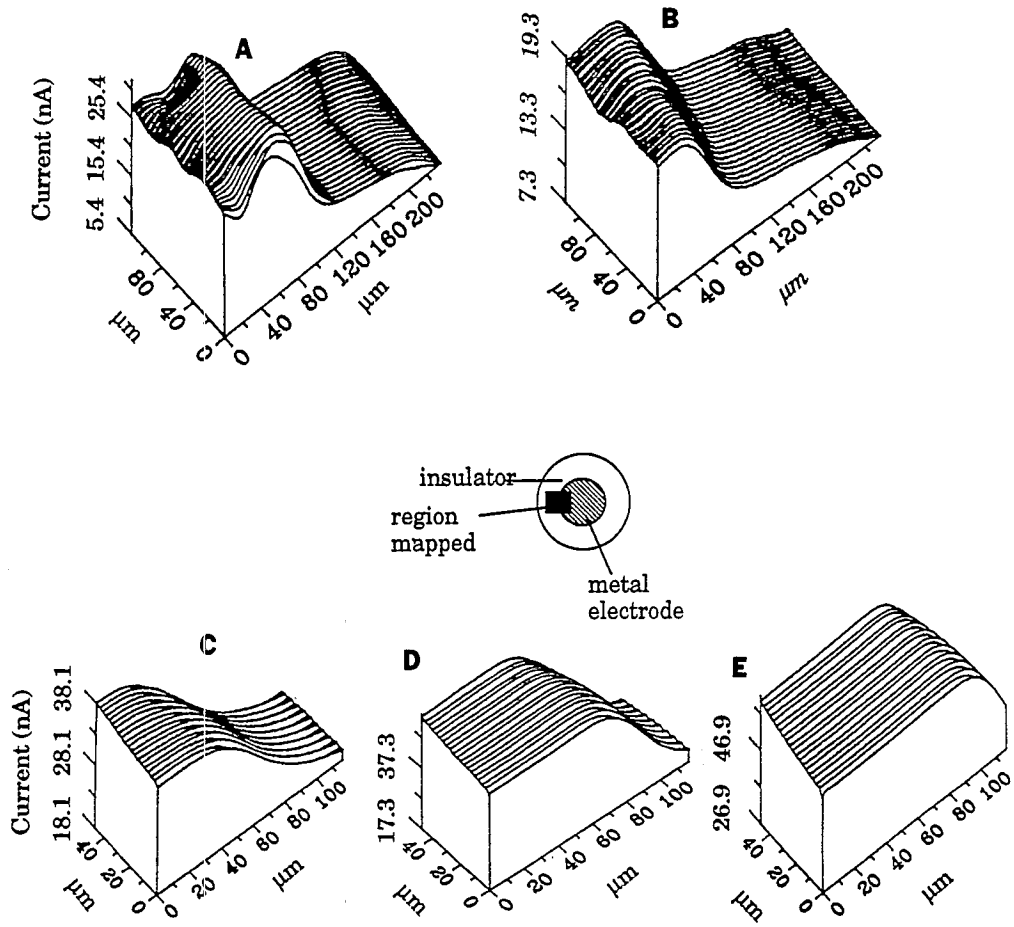


Fig. 17. SECM image of a film on a Au electrode at the Au/glass boundary in MeCN with 0.1 M (TBA)$BF_4$ and 0.76 mM TMPD. (A) Before electrochemical experiment. (B) Reduced film. Tip, 25 μm-dia. Pt; $i_{T,\infty}$ = 14-5 nA. SECM image of a film on a Pt electrode at the Pt/Teflon boundary in MeCN with 0.1 M (TBA)$BF_4$ and 1.8 mM TMPD. The potential was held after the first reduction wave of $C_{60}$. (C) Before electrochemical experiment. (D) After 10 min. (E) After 35 min. Tip, 25 μm-dia. Pt; $i_{T,\infty}$ = 30.7 nA. Reprinted with permission from Ref. [6]. Copyright 1992 American Chemical Society.

### 4.3. Laser-desorption mass spectrometry (LDMS)

LDMS of $C_{60}$ films allows the ex-situ determination of what ions remain in the film after electrochemical cycling. Reduced films showed only $TBA^+$ in the positive ion collection mode and $C_{60}^-$ in the negative ion collection mode [7]. Complete reoxidation of the film showed some trapped $TBA^+$ ion within the film with a much smaller amount of $PF_6^-$. The explanation for this result is still not clear. Two different areas of the

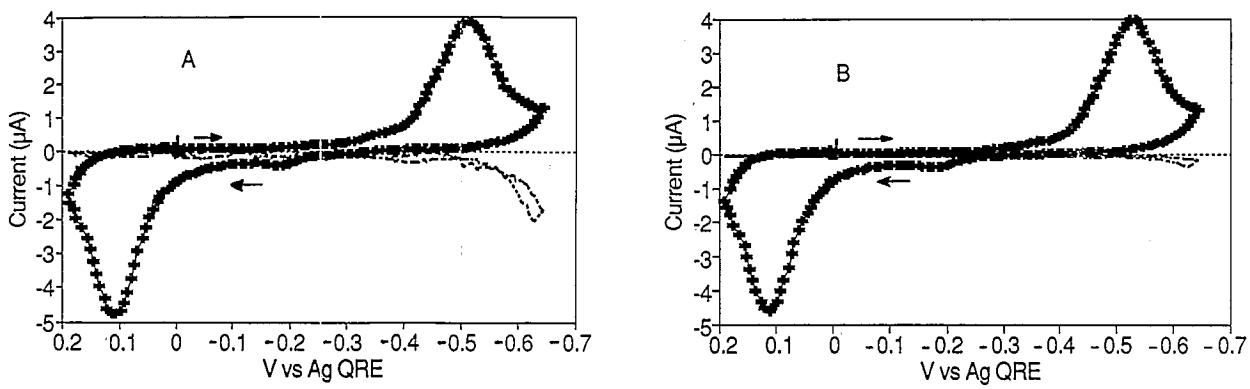


Fig. 18. SECM image of a $C_{60}$ film on a 1 mm-dia. Au electrode. +, Substrate current, cycled over the first pair of waves; – – –, tip current. The potential of the tip was held at 0.3 V vs. AgQRE (silver quasi-reference electrode). Solution, 0.1 M (TBA)$PF_6$ and 10 mM Fc (ferrocene); tip, 10 μm-dia. Pt. The film was cast from a $C_{60}/CH_2Cl_2$ solution. (B) Same as (A) after 10 cycles over the first pair of waves. Reprinted with permission from Ref. [6]. Copyright 1992 American Chemical Society.

Table 1
Solubility of fullerene films upon reduction in MeCN

| Cation | $C_{60}^-$ | $C_{60}^{2-}$ | $C_{60}^{3-}$ | $C_{60}^{4-}$ | $C_{60}^{5-}$ |
|---|---|---|---|---|---|
| *In MeCN* | | | | | |
| $Li^+$ | vs | vs | | | |
| $Na^+$ | vs | vs | | | |
| $K^+$ | vs | vs | vs | | |
| $Cs^+$ | vs | vs | insol. | | |
| $Ca^{2+}$ | sl. s | vs | vs | | |
| $Ba^{2+}$ | s | | | | |
| $TEA^+$ | sl. s | s | s | | |
| $TBA^+$ | sl. s | s | s | | |
| $THA^+$ | insol. | | | | |
| $TOA^+$ | insol. | | | | |
| $M(bpy)_3^{2+}$ | insol. | | | | |
| *In $NH_3$* | | | | | |
| $K^+$ | vs | vs | vs | vs | insol. |

vs, very soluble; s, mostly soluble; sl. s, partially soluble; insol., insoluble.

non-uniform $C_{60}$ film were used for positive and negative ion collection; some $C_{60}$ might be isolated from the electrode and thus might not be fully reoxidized.

### 4.4. Surface-enhanced Raman spectroscopy (SERS)

SERS was used to examine $C_{60}$ and ($\eta^5$-$C_9H_7$) $Ir(CO)(\eta^2$-$C_{60})$ electroactive films in MeCN [8, 9]. A comparison of the SER spectra was used to observe the effect of "symmetry lowering". For $C_{60}$, 14 SER peaks were seen, including four normally forbidden infrared-active peaks. The selection rule is relaxed for these peaks, a common feature of SERS. After forming a $C_{60}^-$ film by electroreduction, a symmetry-lowering effect was observed as various symmetric band peaks were downshifted, intensified, and split. This downshift was a function of the supporting electrolyte cation, and the effects of $Li^+$, $Na^+$, $K^+$, $TEA^+$, $TBA^+$, and $Ph_4As^+$ were reported. No mention of the role the cations play in dissolution was made. The smaller cations downshifted the frequency of $C_{60}^-$ more than the larger ones, and this was attributed to larger perturbations of the fullerene lattice containing smaller counter cations. The Ir–$C_{60}$ showed similar behavior, which showed that the reduction of the complex was fullerene-localized [9].

## 5. Electrolyte effects on the electrochemistry of $C_{60}$ films

The effect of the supporting electrolyte on the electrochemistry of $C_{60}$ thin films has been addressed by many groups. The supporting electrolyte cation plays a strong role in both film structural changes and solubility when a fullerene film is reduced (Table 1). By far, the most studied cation has been $TBA^+$, but alkali and alkaline earth metal cations, other tetra-n-alkylammonium cations, and larger metal-complex cations have also been used. In contrast, the supporting electrolyte anion seems to have little or no effect on the electrochemistry.

### 5.1. Alkali and alkaline earth metal cations

The main effect of small metal cations is dissolution of the fullerene film upon reduction, resulting in an unstable film electrochemistry. Another important effect is the extremely small potential separation between successive reductions of the fullerene film, possibly resulting from the large overpotential to reach the first reduction followed by more facile reductions to $C_{60}^{2-}$ and $C_{60}^{3-}$ in solution. Finally, the peak splittings between cathodic and anodic peaks are found to be much smaller with $Li^+$, $K^+$, and $Cs^+$ than with $TBA^+$ [6].

$Li^+$ electrolytes are the most popular alkali electrolytes in the literature of $C_{60}$ films. Several electrochemical studies showed that the film quickly loses its initial reduction behavior after the first couple of voltammetric cycles [6, 13, 14]. This is a direct result of dissolution of the film, as confirmed with EQCM results [14] (Section 4.1). The SERS of $C_{60}$ and Ir–$C_{60}$ complex films [9] showed the largest frequency shift for film reduction with a lithium electrolyte. Other studies have looked at lithium polymer electrolytes [26] and other possibilities for $C_{60}$ in lithium battery work [15]. Conductivity of partially reduced $C_{60}$ is not enhanced in lithium electrolyte as was the case for $TBA^+$ [10]; this was attributed to lithium's small size, but it is possibly a result of increased dissolution of the reduced $C_{60}$ compared with $TBA^+$.

$Na^+$ electrolytes showed a rapid decrease in the amount of film reduction upon cycling [5, 13, 14]. Jehoulet et al. [5] gave no reason for this instability, Compton et al. [13] attributed it to an irreversible intercalation forming a $NaC_{60}$ salt, and Tatsuma et al. [14], using EQCM (Section 4.1), found that film dissolution dominated and not irreversible intercalation. Zhang et al. [9] observed the SERS spectrum of reduced $C_{60}$ and Ir–$C_{60}$ complex films using a $Na^+$ electrolyte and found a smaller frequency shift than for $Li^+$.

$K^+$ electrolytes show a very small potential spacing between the first three reduction waves of $C_{60}$ films [6]. Two anodic waves are present, with the first oxidation near the reduction potential and the second more positive. Koh et al. [22] expanded on this, showing that $C_{60}$ films formed from the oxidation of $C_{60}^{2-}$ in solution are completely soluble when reduced in a two-electron wave, but that two forms of $C_{60}$ film may be produced by the oxidation. A similar SERS shift was observed for reduced $C_{60}$ and Ir–$C_{60}$ complex films in $K^+$ and $Na^+$ [9].

$Cs^+$ is very similar in its behavior to $Na^+$ and $K^+$ in the first few reductions of $C_{60}$ films [5, 6, 22]. However,

Koh et al. [22] noted that the third reduction of $C_{60}$ results in a marked decrease in solubility of the $C_{60}$, forming a $Cs_3C_{60}$ salt as a precipitate on the electrode (see Fig. 13). Thus, $C_{60}$ and $C_{60}^{3-}$ are insoluble, while $C_{60}^{-}$ and $C_{60}^{2-}$ are very soluble.

The only results using calcium hexafluorophosphate as an electrolyte [22] showed the first and second reduction waves to have very similar potentials, with the $C_{60}$ anions being soluble. A slow precipitation of $Ca^{2+}(C_{60}^{-})_2$ occurs when the potential is held where $C_{60}^{-}$ is produced. Compton et al. [13] proposed an irreversible intercalation of $Ba^{2+}$ into the $C_{60}$ film upon the first reduction, similar to their claims for $Na^+$ and $Li^+$. In light of the EQCM work of Tatsuma et al. [14] with $Na^+$ and $Li^+$, which shows dissolution rather than "irreversible intercalation", it is likely that dissolution also occurs with $Ba^{2+}$. $Ba^{2+}$ should be similar in behavior to $Ca^{2+}$, although the larger size of $Ba^{2+}$ might lead to more insolubility.

### 5.2. Tetra-n-alkylammonium cations

$TBA^+$ studies dominate this area, with 16 literature references, but the ethyl, hexyl, and octyl equivalent cations have also been studied. In general, these cations give films that show decreased dissolution of the film as the cation size is increased. The increased stability of the film results in a structural reorganization within the film which allows the large counter cation into the film and maintains charge neutrality.

The complex nature of the reduction waves of $C_{60}$ films with $TBA^+$ has been the subject of many papers. $TEA^+$ is smaller than $TBA^+$, and therefore is reported to form a less stable film with increased dissolution [5, 6]. The peak splitting for the cathodic and anodic waves is only 400 mV compared with 560 mV with $TBA^+$, suggesting increased solubility and less structural reorganization in the remaining $TEA^+$-doped film [6]. Compton et al. [13] also reported the CV for $TEA^+$ electrolyte showed a smaller peak separation.

$THA^+$ and $TOA^+$ produce more stable films than $TBA^+$, as reflected in the higher reduction charge ratio (second reduction charge/first reduction charge) [5, 6]. This indicates much less dissolution of the film with larger cations and more cation incorporation and results in much broader waves for $TOA^+$ after the first cycle [6]. Compton et al. [13] also reported the initial CV for $THA^+$ and $TOA^+$ and attributed the behavior to the electrochemical intercalation into the $C_{60}$ film.

### 5.3. Other large cations

The results of studies using $TOA^+$ suggest that larger cations may lead to more stable films. The two large-cation systems in the literature are metal–bipyridyl complex cations and tetraphenylarsonium or phosphonium cations. Dissolution of the film is negligible in these systems, and cation incorporation with structural reorganization is the main process.

Miller and Rosamilia [24] formed an insoluble $C_{60}^{-}$ doped film with either $Ph_4P^+$ or $Ph_4As^+$ by the reduction of $C_{60}$ in *o*-dichlorobenzene (ODCB). $C_{60}$ is soluble in ODCB, but upon reduction, electrocrystallization of $Ph_4P^+C_{60}^{-}$ occurs. This film was transferred to an ODCB/$TBA^+$ solution for rotating ring disk electrode studies. The reduction of this film generated soluble $C_{60}^{2-}$ detected at the ring electrode. The oxidation of this film generated soluble $C_{60}$, although the behavior indicated a complex stepwise process [24].

In our most recent work in this area, metal–bipyridyl complex salts such as $M(bpy)_3^{2+}(PF_6)_2$, where M is Ni, Cd, Zn, or Fe, have been studied as electrolytes for the reduction of $C_{60}$ films [30]. In this case, the films are very stable, EQCM results show that no dissolution occurs (Fig. 15), and charge balance is maintained by cation incorporation in the first reduction scan. In following scans, a balance of cation ejection/anion incorporation occurs, with EQCM results showing the final film mass significantly greater than the initial mass. This indicates that both cation and anion are trapped within the $C_{60}$ film upon cycling. The lower solubility of these complexes in MeCN may play a role in the ability of the film to concentrate electrolyte out of solution into a film upon cycling.

## 6. Mechanism and applications of $C_{60}$ film electrochemistry

### 6.1. Proposed mechanism

A key feature of the electrochemistry of $C_{60}$ (and $C_{70}$) films is the sharp peaks and large peak splitting found between reduction and reoxidation peaks (Fig. 2(b),A). Typically, especially if the electron-transfer reaction rate is rapid, films on electrodes are characterized by parabolic peaks with a peak width at half-height of about 91 mV ($n = 1$) and the same peak potentials for the cathodic and anodic peaks ($\Delta E = 0$). The large peak splitting observed with $C_{60}$ has been ascribed to large structural changes that occur in the solid $C_{60}$ lattice during reduction and incorporation of the cation [5, 6], as represented by Scheme 1, where A and B represent different film structures, with A being characteristic of the initial $C_{60}$ lattice and B that of the equilibrium $M^+C_{60}^{-}$ lattice. Similar behavior has been seen with films of the solid electronic conductor TTF–TCNQ (tetrathiafulvalence–tetracyanoquinodimethane) and related materials [33–35].

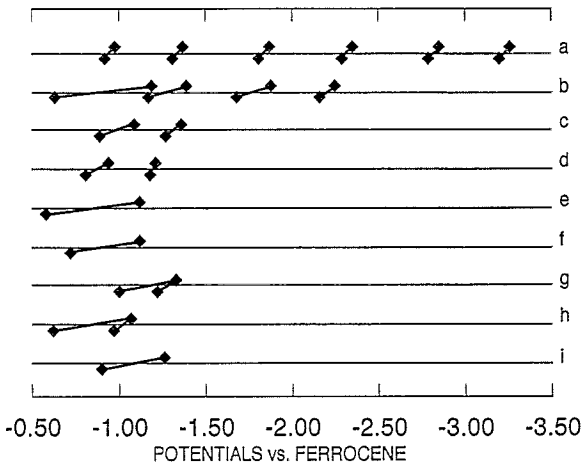


Fig. 19. Comparison of reduction peak potentials and corresponding reoxidation potentials: (a) solution of $C_{60}$ MeCN/toluene mixture, (b) $C_{60}$ film with TBAP electrolyte, (c) LB $C_{60}$ film with $(TBA)BF_4$ electrolyte, (d) LB $C_{60}$: arachidic acid 1:1 film with $(TBA)BF_4$; $C_{60}$ film with (e) $(TOA)AsF_6$, (f) $(TEA)AsF_6$, (g) $CsAsF_6$, (h) $KPF_6$, and (i) $LiAsF_6$ electrolytes.

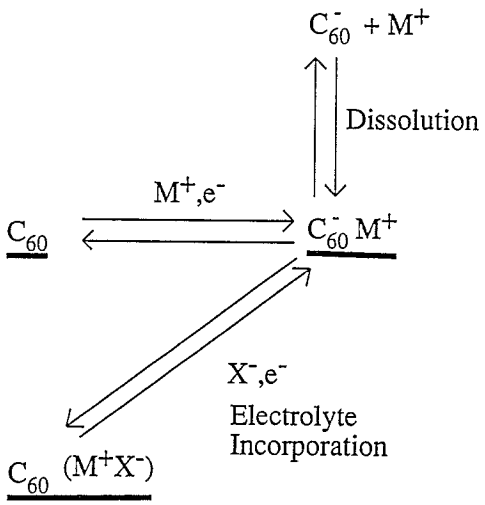


Fig. 20. The first reduction processes of a $C_{60}$ film with $TBA^+$.

$$\begin{array}{ccc} (C_{60})_A + M^+ + e^- & \rightleftarrows & (M^+C_{60}^-)_A \\ \uparrow \text{fast} & & \downarrow \text{fast} \\ (C_{60})_B + M^+ + e^- & \rightleftarrows & (M^+C_{60}^-)_B \end{array}$$

**Scheme 1**

A general feature of all of the electrochemical data gathered to date is a rough correlation between the size of the doping cation and the peak splitting. In general, the larger the doping cation, the larger the peak splitting. This is shown in Fig. 19, where the peak potentials determined for all of the studied processes are presented along with the peak potentials determined for dissolved $C_{60}$. Such a correlation appears consistent with the proposed model, since injecting a large cation into the $C_{60}$ phase would be accompanied by more significant structural changes than injecting a small cation that could occupy interstitial space in the $C_{60}$ lattice. The electrochemical behavior of the LB films seems to be concordant with that concept, since the films consisting of one or a few monolayers show little peak splitting. However, in addition to the properties of the pure $C_{60}$ phase and the doping cations, dissolution of the reduced phase can affect the observed electrochemistry (see Table 1). Thus the model is most appropriate for quaternary ammonium, phosphonium, arsonium, and metal–bipyridyl complex electrolytes.

The results of Koh et al. [22] do show the existence of two different forms of $C_{60}$ films electrogenerated in $KPF_6$ and $CsAsF_6$ solutions. Moreover, the composition of $C_{60}$ films formed with $(TBA)ClO_4$ as background electrolyte depend upon the conditions of formation (e.g., scan rate, concentration) [22]. Irreversible cation trapping has also been suggested to contribute to the large peak splitting in the $TBA^+$ solutions [7]. Significant electrical resistance of the pure $C_{60}$ and $(TBA^+)$ $(C_{60}^-)$ [6, 10] can itself generate a large hysteresis, as shown by Gottesfeld et al. [36]. Note, however, that the electrochemically irreversible (i.e., occurring with a large overpotential) intercalation of $TBA^+$ and other cations is unusual, as mentioned in Section 3.1. This unusual character is reflected not only by exceptionally narrow reduction and oxidation peak widths, but also by a weak [6], if any [12], dependence of the peak potentials on the scan rate. Such behavior can be predicted for a system that is characterized by a so-called N-shaped free energy function [37]. The simplest electrochemical example of such a function is the Frumkin adsorption isotherm [38–41], with an interaction parameter $g > 4$, i.e. for extremely strong attractive interactions within the adsorbed layer. A system characterized by an N-shaped free energy function can undergo both reversible and irreversible transformations [37]. For irreversible electrochemical transforma-

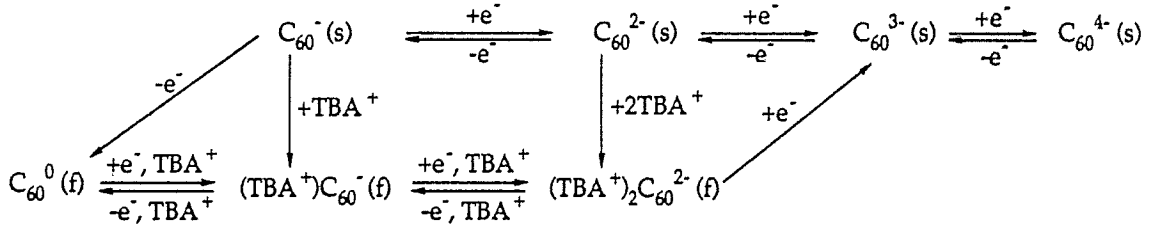


Fig. 21. Extended scheme of $C_{60}$ film reduction in $TBA^+$. Reprinted with permission from Ref. [22]. Copyright 1993 American Chemical Society.

tions, a large peak splitting is expected that cannot be removed, even at the slowest scan rates possible, because the splitting is determined by the nodes of the energy function. In addition, for a perfect system, the transition from one state to another occurs instantly, producing spike-like reduction and oxidation peaks. The overall mechanism on cycling should also include the possibility of dissolution and the incorporation of electrolyte into the film, as shown by EQCM studies. A general picture for the first reduction is shown in Fig. 20. This type of scheme can then be extended to include additional electron-transfer steps, e.g. as proposed for $TBA^+$ [22] (Fig. 21).

### 6.2. Possible electrochemical applications

Several applications have been suggested for fullerene films, although none is yet nearing practicality. Intercalation of alkali metals (e.g. $Li^+$) into fullerene films could find application as the anode in rechargeable (secondary) batteries. However, improvement in the stability of the original and reduced films and in the reversibility of the electrochemical processes is needed. Initial results with $Li^+$ [15, 26], described above, have not been encouraging. Similarly, "hydrogen storage", in the form of either adsorbed hydrogen or hydrogenated fullerenes, has been suggested. Again, stability and reversibility difficulties have yet to be overcome. Photoelectrochemical effects have also been observed with $C_{60}$ films [11]; however, the efficiency of these (electrons generated per incident photon) was rather low.

## 7. Summary

The electrochemical reduction steps in $C_{60}$ films are more complicated processes than those for the corresponding dissolved species. Film reduction involves several factors: counter ion (cation) transport into the film, significant structural rearrangements on reduction and reoxidation, resistivity changes, and dissolution. These depend upon the nature of the contacting solution (solvent, electrolyte) and the conditions used to form the film. Most studies have been carried out with solvent-cast films of $C_{60}$ in solutions of alkali metal, alkaline earth, or quaternary ammonium salts in MeCN. A summary of the proposed mechanism for the first redox step ($C_{60}/C_{60}^-$) is shown in Fig. 20. Upon reduction of the $C_{60}$ crystals, cations are incorporated into the film with a change in structure to accommodate these counter ions. Some dissolution can occur, since the reduced forms of $C_{60}$ are more soluble in MeCN. Upon reoxidation, cations are expelled and electrolyte anions are incorporated, producing a $C_{60}$ film containing some electrolyte. Some $C_{60}$ can also be redeposited from dissolved species. The relative contribution from dissolution is larger with smaller cations such as $Na^+$. The reactions that occur during additional reduction steps for the tetra-n-butylammonium counter ion are shown in Fig. 21. Again dissolution, electrolyte incorporation, and film reorganization occur during the redox processes.

The most striking characteristic of the cyclic voltammograms of $C_{60}$ films is the unusual irreversibility of the waves manifested by a large splitting between the reduction and reoxidation waves and the very narrow peaks observed (see Figs. 2(b) and 3). This behavior has been explained (qualitatively) in terms of structural rearrangement upon incorporation of ions. However, a quantitative model based on defined parameters (standard potentials, diffusion coefficients, rate constants) is not yet available, and simulation of the experimental voltammograms over a range of scan rates has not yet been reported.

## Acknowledgements

The support of this work by the National Science Foundation and the Robert A. Welch Foundation is gratefully acknowledged. This material is based in part upon work supported under a National Science Foundation Graduate Research Fellowship (D.E.C.).

## References

[1] D. Dubois, K. M. Kadish, S. Flanagan and L. J. Wilson, *J. Am. Chem. Soc., 113* (1991) 7773.
[2] Q. Xie, E. Pérez-Cordero and L. Echegoyen, *J. Am. Chem. Soc., 114* (1992) 3978.
[3] Y. Ohsawa and T. Saji, *J. Chem. Soc., Chem. Commun.*, (1992) 781.
[4] Q. Xie, F. Arias and L. Echegoyen, *J. Am. Chem. Soc., 115* (1993) 9818.
[5] C. Jehoulet, A. J. Bard and F. Wudl, *J. Am. Chem. Soc., 113* (1991) 5456.
[6] C. Jehoulet, Y. S. Obeng, Y.-T. Kim, F. Zhou and A. J. Bard, *J. Am. Chem. Soc., 114* (1992) 4237.
[7] F. Zhou, S. L. Yau, C. Jehoulet, D. A. Laude, Z. Gaun and A. J. Bard, *J. Phys. Chem., 96* (1992) 4160.
[8] Y. Zhang, G. Edens and M. J. Weaver, *J. Am. Chem. Soc., 113* (1991) 9395.
[9] Y. Zhang, Y. Du, J. R. Shapley and M. J. Weaver, *Chem. Phys. Lett., 205* (1993) 508.
[10] M. Nishizawa, T. Matsue and I. Uchida, *J. Electroanal. Chem. Interfacial Electrochem., 353* (1993) 329.
[11] B. Miller, J. M. Rosamilia, G. Dabbagh, R. Tycko, R. C. Haddon, A. J. Muller, W. Wilson, D. W. Murphy and A. F. Hebard, *J. Am. Chem. Soc., 113* (1991) 6291.
[12] R. G. Compton, R. A. Spackman, R. G. Wellington, M. L. H. Green and J. Turner, *J. Electroanal. Chem. Interfacial Electrochem., 327* (1992) 337.
[13] R. G. Compton, R. A. Spackman, D. J. Riley, R. G. Wellington, J. C. Eklund, A. C. Fisher, M. L. H. Green, R. E. Doothwaite, A. H. H. Stephens and J. Turner, *J. Electroanal. Chem. Interfacial Electrochem., 344* (1993) 235.

[14] T. Tatsuma, S. Kikuyama and N. Oyama, *J. Phys. Chem.*, *97* (1993) 12067.
[15] L. Seger, L.-Q. Wen and J. B. Schlenoff, *J. Electrochem. Soc.*, *138* (1991) L81.
[16] J. L. Wragg, J. E. Chamberlain, H. W. White, W. Krätschmer and D. R. Huffman, *Nature (London), 348* (1990) 623.
[17] T. Atake, T. Tanaka, H. Kawaji, K. Kikuchi, K. Saito, S. Suzuki, Y. Achiba and I. Ikemoto, *Chem. Phys. Lett.*, *196* (1992) 321.
[18] J. Milliken, T. M. Keller, A. P. Baronavski, S. W. McElvany, J. H. Callahan and H. H. Nelson, *Chem. Mater.*, *3* (1991) 386.
[19] L. O. S. Bulhões, Y. S. Obeng and A. J. Bard, *Chem. Mater.*, *5* (1993) 110.
[20] L. M. Goldenberg, G. Williams, M. R. Bryce, A. P. Monkman, M. C. Petty, A. Hirsch and A. Soi, *J. Chem. Soc., Chem. Commun.*, (1993) 1310.
[21] W. Koh, D. Dubois, W. Kutner, M. T. Jones and K. M. Kadish, *J. Phys. Chem.*, *96* (1992) 4163.
[22] W. Koh, D. Dubois, W. Kutner, M. T. Jones and K. M. Kadish, *J. Phys. Chem.*, *97* (1993) 6871.
[23] C. A. Foss, D. L. Feldheim, D. R. Lawson, P. K. Dorhout, C. M. Elliott, C. R. Martin and B. Parkinson, *J. Electrochem. Soc.*, *140* (1993) L84.
[24] B. Miller and J. M. Rosamilia, *J. Chem. Soc., Faraday Trans.*, *89* (1993) 273.
[25] F. Zhou, C. Jehoulet and A. J. Bard, *J. Am. Chem. Soc.*, *114* (1992) 11004.
[26] Y. Chabre, D. Djurado, M. Armand, W. R. Ramanow, N. Coustel, J. P. McCauley, J. E. Fischer and A. B. Smith, *J. Am. Chem. Soc.*, *114* (1992) 764.
[27] K. Meerholz, P. Tschuncky and J. Heinze, *J. Electroanal. Chem. Interfacial Electrochem.*, *347* (1993) 425.
[28] A. J. Bard and L. R. Faulkner, *Electrochemical Methods, Fundamentals and Applications*, Wiley, New York, 1980.
[29] C. Jehoulet and A. J. Bard, *Angew. Chem., Int. Ed. Engl.*, *30* (1991) 836.
[30] D. Cliffel, J. Chlistunoff and A. J. Bard, unpublished work.
[31] See, e.g., D. A. Buttry, in A. J. Bard (ed.), *Electroanalytical Chemistry*, Vol. 17, Marcel Dekker, New York, 1991, p. 1.
[32] A. J. Bard, F.-R. F. Fan and M. V. Mirkin, in A. J. Bard (ed.), *Electroanalytical Chemistry*, Vol. 18, Marcel Dekker, New York, 1994, p. 243.
[33] C. D. Jaeger and A. J. Bard, *J. Am. Chem. Soc.*, *101* (1979) 1690.
[34] C. D. Jaeger and A. J. Bard, *J. Am. Chem. Soc.*, *102* (1980) 8435.
[35] T. P. Henning and A. J. Bard, *J. Electrochem. Soc.*, *130* (1983) 613.
[36] S. Gottesfeld, A. Redondo, I. Rubinstein and S. W. Feldberg, *J. Electroanal. Chem. Interfacial Electrochem.*, *265* (1989) 15.
[37] S. W. Feldberg and I. Rubinstein, *J. Electroanal. Chem. Interfacial Electrochem.*, *240* (1988) 1, and references therein.
[38] E. Laviron, *J. Electroanal. Chem. Interfacial Electrochem.*, *63* (1975) 245.
[39] E. Laviron, *J. Electroanal. Chem. Interfacial Electrochem.*, *100* (1979) 263.
[40]. A. Sadkowski, *J. Electroanal. Chem. Interfacial Electrochem.*, *208* (1986) 69.
[41] A. Sadkowski, *J. Electroanal. Chem. Interfacial Electrochem.*, *210* (1986) 21.